Impact of reflective torque tube on rear side irradiance in bifacial photovoltaic modules

Trevor J. Coathup[a], Mandy R. Lewis[a], Annie C. J. Russell[a], Alejandro Conesa[b], Javier Guerrero-Perez[b], Christopher E. Valdivia[a], Karin Hinzer[a]
[a]SUNLAB, Centre for Research in Photonics, University of Ottawa, Ottawa, ON, Canada
[b]Soltec Innovations, Murcia, Spain

ABSTRACT

Non-uniform irradiance on the rear side of bifacial photovoltaic (PV) modules causes electrical mismatch between cells and energy loss across the module. Racking structures increase this non-uniformity through shadows and reflections that vary throughout the day. However, commercial software typically use constant values to estimate mismatch losses in annual simulations.

We investigate the impact of torque tube shading and reflection on rear side irradiance mismatch in bifacial PV modules in one-in-portrait (1P) and two-in-portrait (2P) horizontal single-axis trackers with a range of ground albedos over a typical meteorological year in Livermore, California, USA. Irradiance simulations use a version of bifacial_radiance, the National Renewable Energy Laboratory's python wrapper for the RADIANCE ray tracing software, which we modified for arbitrary 2D irradiance sampling of the module(s) under investigation.

For a torque tube reflectivity of 0.745, torque tube reflection accounts for 3.0% and 5.5% of the annual rear insolation in 1P and 2P configurations, respectively, for a 0.2 albedo; or 2.9% and 3.1% for a 0.6 albedo. Torque tube reflection decreases annual rear insolation mismatch from 11.8% to 10.7% in 1P configurations, and from 11.5% to 9.8% in 2P configurations with 0.2 albedo. Similarly, with 0.6 albedo, annual rear insolation mismatch decreases from 12.6% to 11.6% in 1P configurations, and from 11.9% to 10.4% in 2P configurations. However, we demonstrate that annual figures are insufficient for capturing the impact of torque tube reflection; seasonal and diurnal variations must also be considered.

Keywords: Annual energy yield modelling, ray tracing, single axis tracking, silicon module, rear shading, global irradiance, ground albedo, PV system racking

1. INTRODUCTION

Bifacial photovoltaics (PV) are becoming an increasingly important segment of the silicon photovoltaics industry, with bifacial PV predicted to make up 80% of the market share within the next ten years [1]. Single-axis tracking (SAT) systems can further increase energy yield by rotating the modules throughout the day, typically from east to west, thereby maximizing illuminated cross-sectional area, and reducing cosine and angle-of-incidence losses [2]. Pairing these two technologies can reduce the levelized cost of energy (LCOE), improving the cost-competitiveness of bifacial PV [3]. To hasten the adoption of these technologies across a wider range of deployment conditions and system configurations, accurate energy yield predictions are essential to reduce investment risk and increase investor confidence [4]. However, bifacial energy yield models are still undergoing development and validation, and their uncertainty may act as a barrier to adoption [4].

One of the challenges of bifacial PV performance modelling is accurately accounting for the effects of racking elements on the rear irradiance. Most SAT systems have rows of PV modules rotating around a torque tube (TT) that runs the length of the row, but the system configuration can impact rear irradiance and, as a result, energy yield. For example, SAT two-in-portrait (2P) modules, where one module is mounted on each side of the torque tube, show higher bifacial gain than one-in-portrait (1P) modules, where the torque tube runs behind the center of the single module [5]. Some optical models, such as ray tracing models, can represent mounting structures and account for light blocked or reflected by the torque tube on specific parts of the PV module. However, it is more common for simplified bifacial PV performance models to

represent racking shading by a constant rear shading factor applied to reduce the total energy yield at the end of the calculation [6]. Torque tube shading can cause reduced and non-uniform irradiance leading to increased electrical mismatch and reduced total energy yield output [7]–[9]. In addition, constant shading factors applied to bifacial PV performance models do not typically account for light that is reflected from the torque tube. Torque-tube-reflected light can increase rear-side irradiance, and consequently energy yield, with approximately 1% electrical mismatch loss [9]. The isolated impact of torque tube reflection on rear irradiance mismatch is not widely reported in the literature.

In this work, we model the central module rear-side irradiance of comparable 1P and 2P North-South horizontal SAT bifacial systems. For modules in 1P and 2P configurations, we quantify the impact of torque tube reflection on the rear irradiance magnitude, 2D profile, and mismatch at 0.2 and 0.6 ground albedo. First, we will describe the model and system configuration. Next, we will outline trends in torque-tube-reflected irradiance on a summer and winter day. Finally, we will show annual effects of torque tube reflection based on time of day and month of year.

2. MODEL DESCRIPTION

The PV systems were modelled in bifacial_radiance [10]–[13], an open-source software by the National Renewable Energy Laboratory (NREL) built around RADIANCE [14], a ray tracing software. For this study, the following modifications were made to bifacial_radiance (version 0.3.4): (1) adjustments to the ray trace settings to improve accuracy, particularly at the module edges near the frame where shading is high; (2) the addition of module frames and module supports to the module under test (Figure 1a, Figure 1b); (3) the removal of torque tube objects from rows not under test; and (4) the implementation of 2D irradiance sampling on the module under test.

In bifacial_radiance, there are two accuracy settings included by default (low and high) that set the parameters for RADIANCE's ray trace method, *rtrace* [15]. The high accuracy method has a longer runtime but results in less noise in the irradiance data than the low accuracy method. In this work, each irradiance value was calculated multiple times (3 times for annual simulations and 10 times for select days), then averaged to reduce the noise. Additionally, the *rtrace* ambient accuracy parameter, *aa*, was altered from the default bifacial_radiance low accuracy option of 0.1 to 0.05 to improve the calculation's accuracy with minimal increase to the computation time.

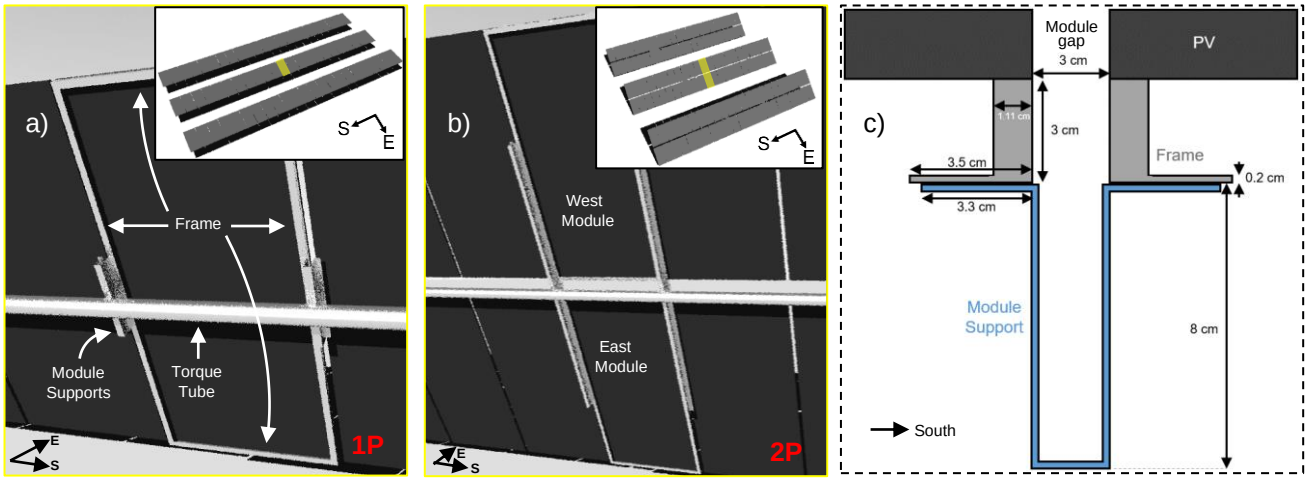

Figure 1. Module supports and frame on the module under test for (a) 1P and (b) 2P modules with a reflective torque tube along the row under test. Overview of the modelled 3 row by 23 module 1P array (a-inset) and 2P array (b-inset) with the central module(s) highlighted. Cross-sectional schematic (c) shows the frame and module support dimensions common for both 1P and 2P looking down the length of the module. Frame dimensions are the same along each of the module edges.

We calculated rear irradiances for the center module(s) of both a 1P and a 2P horizontal SAT system from hourly Typical Meteorological Year (TMY) data for the Bifacial Test Evaluation Center (BiTEC) site in Livermore, California, USA (37.70° N, 121.82° W, 121 m elevation). The scene parameters for the modelled 1P and 2P systems are presented in Table 1. Parameters were chosen to emulate a Soltec 2P tracker and a comparable 1P configuration [16], but with a round torque tube shape rather than square. The 1P system consisted of 3 rows of 23 modules (Figure 1a inset), while the 2P system consisted of 3 rows of 23 sets of 2 side-by-side modules (Figure 1b inset), with the torque tube oriented north-south and parallel to the ground in both systems. Piles were not included in the array geometry because each module is affected differently by pile shading due to their proximity to or distance from a pile. Omitting piles allows the single-module results to be interpreted more generally.

Rather than including a module frame and module supports on every module in the test array, these elements were only included on the module under test, as shown in Figure 1a and b, to decrease computation time. Similarly, the torque tube was only included for the row with the module under test. Detailed frame and module support dimensions are illustrated in Figure 1c. The module supports were positioned between, and directly in contact with, the torque tube and module frame. In single-timestamp benchmarking tests, these simplifications decreased computation time by approximately a factor of 10, while changing total torque-tube-reflected irradiance by 2.6% absolute.

Table 1. Scene parameters used in bifacial_radiance for the 1P and 2P systems.

Scene Parameter	**1P System**	**2P System**
System configuration:		
Modules per row	23	23
Number of rows	3	3
Row pitch	4.8355 m	10 m
Ground cover ratio	0.456	0.456
Piles	Not included	Not included
Ground clearance	1.35 m	2.35 m
Tracking angle range	±60°	±60°
Site configuration:		
Location	Livermore, CA	Livermore, CA
Irradiance data	TMY	TMY
Albedo	0.2 & 0.6	0.2 & 0.6
Module:		
Width	1.032 m	1.032 m
Length	2.205 m	2.205 m
Thickness	0.02 m	0.02 m
Module gap	0.03 m	0.03 m
Module supports:		
Height	0.08 m	0.08 m
Length	0.44 m	2.8 m
Width	0.03 m	0.03 m
Torque tube:		
Torque tube gap	N/A	0.15 m
Shape	Round	Round
Diameter	0.1 m	0.1 m
Reflectivity	0.745 | 0	0.745 | 0
Specularity	0.9	0.9
Roughness	0.2	0.2

Module dimensions emulate the Jinko Solar Tiger Bifacial JKM460M-7Rl3-TV module [17]. They are set as 1.032 m wide and 2.205 m long, with a 0.03 m gap between modules, and a 0.15 m gap between the 2P east and west modules. The row-to-row pitch is set to maintain a ground ratio coverage (GCR) of 0.456: 10 m for the 2P system and 4.8355 m for the 1P system. GCR is defined as a ratio of the collector length to the row-to-row pitch, where the collector length is the width of the module row (including east and west modules and the module gap in the 2P case) [9]. The collector tilt angle is controlled by PVLib's tracking algorithm [18], with a maximum tracking angle of ±60° and backtracking enabled.

To isolate and study torque tube reflection, the rear irradiance of the module under investigation is first sampled in a 2D array of 52x24 points per module face (1248 for 1P, 2496 for 2P) with a reflective torque tube, as shown in Figure 2a. We set the reflective torque tube material to a reflectivity of 0.745, specularity of 0.9, and roughness of 0.2. The module support and module frame were modelled with the same material parameters as the reflective torque tube. The high number of sampling points captures the irradiance and irradiance mismatch effects near the module edges and racking fixtures including the frame, module supports, and torque tube. Next, the simulation is repeated with the torque tube reflectivity set to 0, as shown in Figure 2b. The module support and module frame materials remain reflective in the absorptive torque tube case. The difference between the rear irradiance with a reflective torque tube and the rear irradiance with a fully absorptive torque tube yields the torque tube reflection signal, shown in Figure 2c. While these figures illustrate the 2P rear irradiance values of a single timestamp at noon on a summer sunny day (June 19) with 0.2 ground albedo, the process is identical for each timestamp and albedo, as well as for the 1P module.

Figure 2c shows the torque tube reflection is predominant near the torque tube, and is relatively flat along the North-South direction, illustrated by the cross-sectional averages along the module width (Figure 2d) and along the collector width (Figure 2e). The torque tube reflection profile is only impacted by the frame at the edge nearest the torque tube, even though the frame reduces the total irradiance (Figure 2a and b) throughout the entire perimeter of the modules.

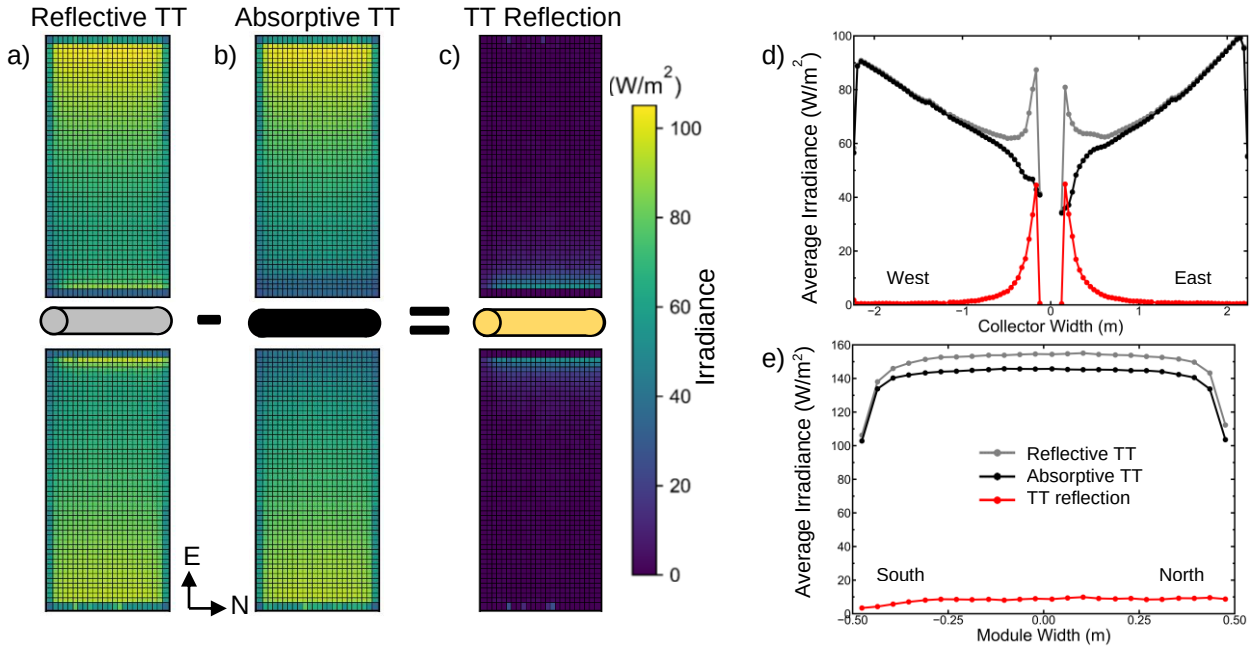

Figure 2. Torque tube (TT) reflection calculation procedure illustrated by 2P rear irradiance values from noon on a summer sunny day. 2D irradiance map of the rear face of the module with (a) a reflective torque tube and (b) an absorbing torque tube. Subtracting (b) from (a) yields (c), a 2D irradiance map of the torque tube reflection. The irradiance averaged along (d) the module width and (e) the module length is plotted for each 2D irradiance map.

3. SIMULATION RESULTS

3.1 Torque-tube-reflected irradiance on a summer and winter day

The torque tube reflection incident on the rear of the module varies over the course of a day and year for both 1P and 2P systems. To illustrate, we show the torque-tube-reflected irradiance on a summer sunny day (June 19), and winter sunny day (December 22) for 1P (Figure 3) and 2P (Figure 4) configurations with 0.2 albedo. The timestamps shown are two hours after sunrise (black, solid line), noon (grey, dashed line), and two hours before sunset (red, dotted line). The morning and evening timestamps shown do not require backtracking.

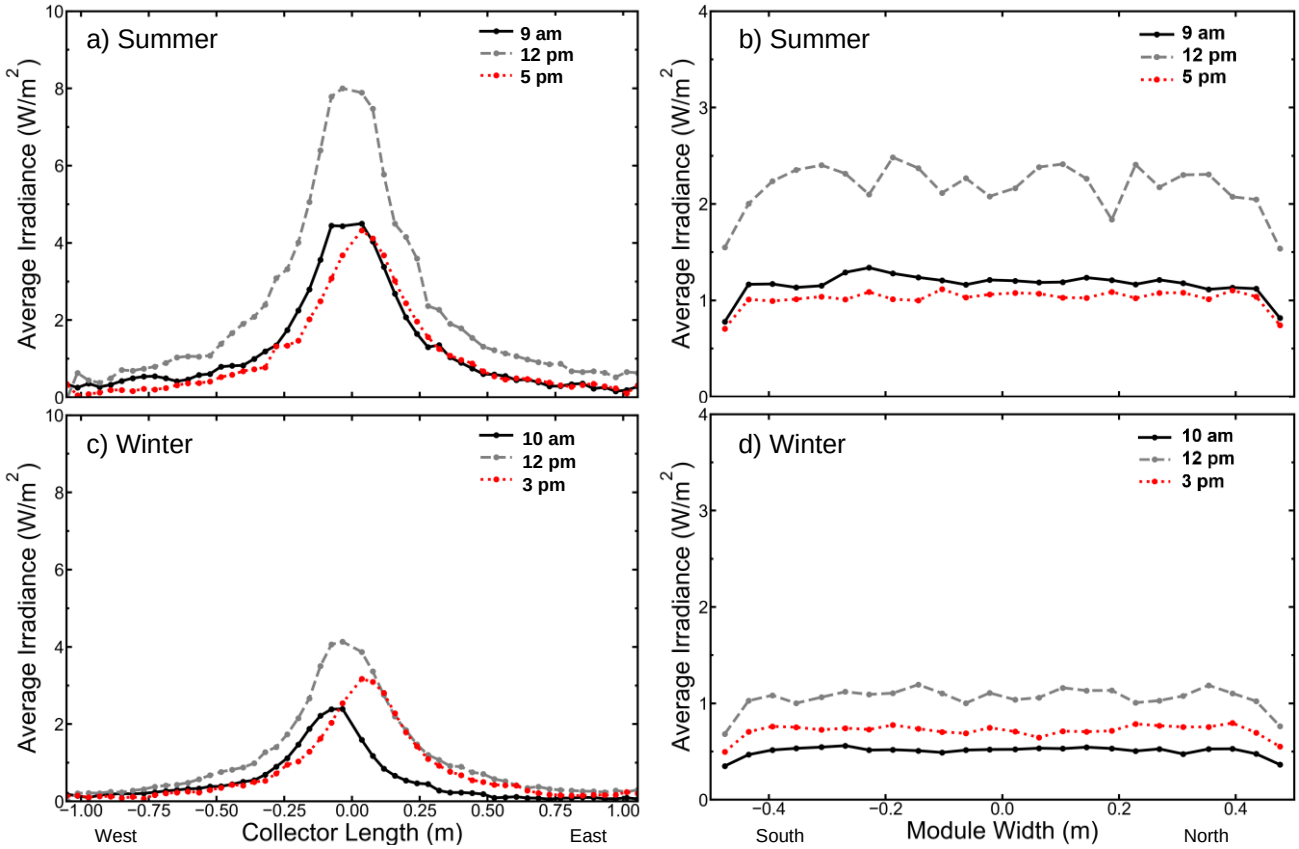

Figure 3. Average torque-tube-reflected irradiance taken along the module width (left), and along the collector length (right), for the 1P configuration with 0.2 albedo, on a summer sunny day (top) and winter sunny day (bottom).

On both the summer (Figure 3a and b) and winter (Figure 3c and d) days, the 1P torque tube reflection is highest in the middle of the day. The irradiance peak is on the western half of the module in the morning and shifts towards the eastern half of the module in the evening as it tracks the sun (Figure 3a and c). The fraction of diffuse and ground-reflected light hitting the torque tube determines which side of the module receives more torque-tube-reflected irradiance. Diffuse light reflects off the torque tube and primarily onto the side of the module higher in the sky (west in the morning; east in the evening), while ground-reflected light incident on the torque tube reflects more strongly onto the side of the panel closer to the ground (east in the morning; west in the evening). Therefore, changing albedo or weather, which can affect the amount of ground-reflected or diffuse light incident on the torque tube, can alter the location of the torque-tube-reflected irradiance peak from east to west along the module. For instance, on the winter day with 0.6 albedo (not shown in Figure

3) and the winter day with 0.2 albedo, the torque-tube-reflected irradiance peak follows the same path across the module throughout both days. However, on the summer day with 0.6 albedo (not shown in Figure 3), the torque-tube-reflected irradiance peak locations are reversed compared to the 0.2 albedo case. This is caused by the higher diffuse irradiance in the winter and the higher ground-reflected irradiance in the summer for this site configuration.

The shift in the peak torque-tube-reflected irradiance from east to west over the course of the day is less significant in the 2P modules with 0.2 albedo (Figure 4a and c). Direct light incident on the front of the torque tube (via the TT gap) increases the 2P torque-tube-reflected irradiance up to nearly 6-times that of the 1P configuration (note the difference in irradiance scales between Figure 3 and Figure 4) and reflects evenly onto the east and west modules during non-backtracking hours. Thus, the shift in peak torque-tube-reflected irradiance from East to West over the day, due to the diffuse and ground-reflected light contributions, is small compared to the total torque-tube-reflected irradiance.

The direct light incident on the torque tube in 2P configurations also impacts the shape of the torque tube reflection signal along the North-South direction (Figure 4b and Figure 4d). The decreased torque-tube-reflected irradiance on the southern side of Figure 4d can be attributed to the module supports shading the southern edge of the module from direct light reflected off the torque tube. During winter in the Northern hemisphere, the sun's low elevation leads the module supports to cast longer shadows on the Southern portion of the torque tube than they do in the summer.

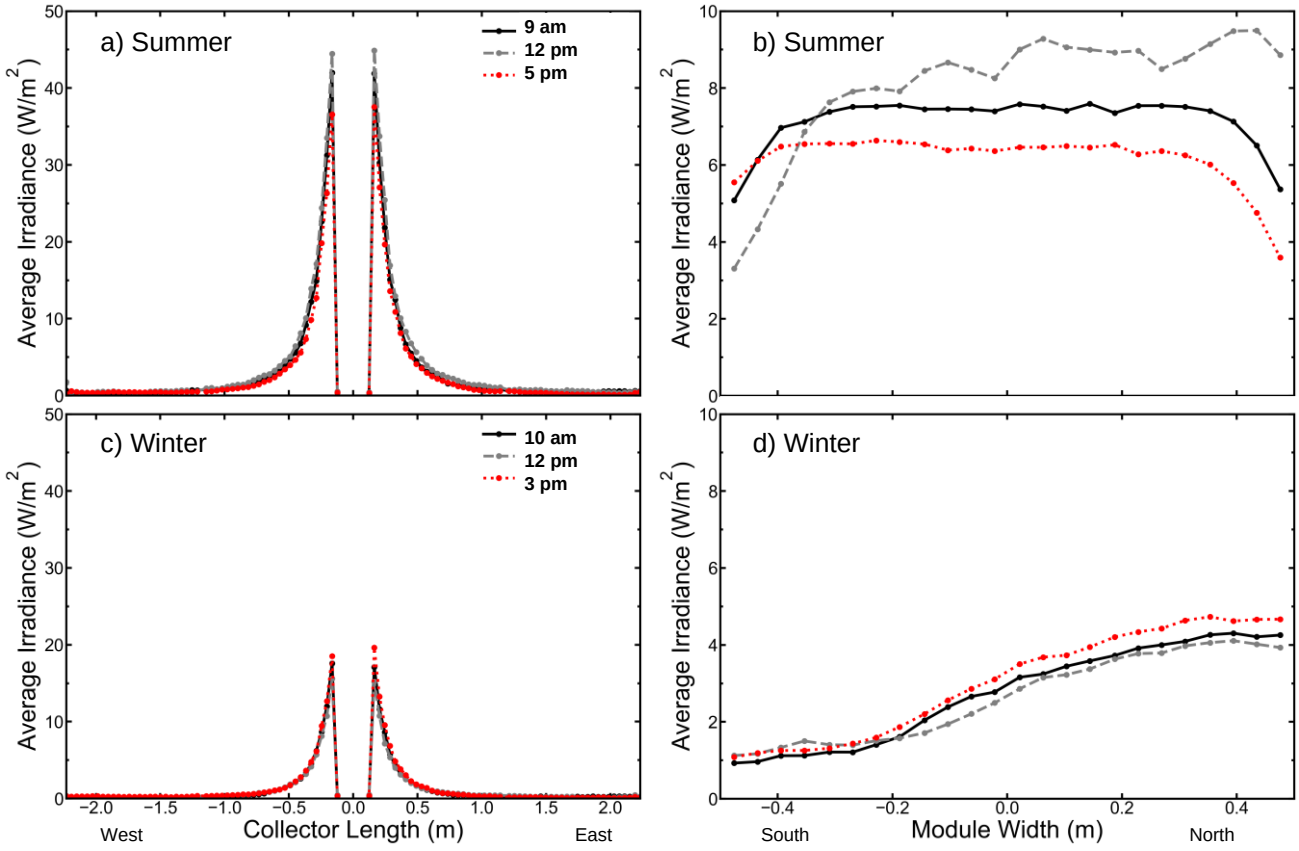

Figure 4.Torque tube reflection for a summer sunny day (top) and winter sunny day (bottom) on a pair of 2P modules with 0.2 albedo. Average torque-tube-reflected irradiance taken along the module width (left), and along the module length (right).

3.2 Hourly impact of torque tube reflection

We investigated each hour of the day separately by calculating an hour-wise annual average torque-tube-reflected irradiance map for each non-zero irradiance timestamp for both 1P (Figure 5a) and 2P (Figure 5b) systems. In the 2P case,

the torque tube is not shaded by the modules and direct irradiance that passes through the torque tube gap illuminates the torque tube and can be reflected to the rear of the module, resulting in higher torque-tube-reflected irradiance. In the 1P case, by comparison, most light incident on the torque tube is ground-reflected and diffuse light, resulting in lower total torque-tube-reflected irradiance. These effects are illustrated by the difference in irradiance scales for each configuration (comparing Figure 5a and b), with 2P peak torque-tube-reflected irradiance reaching nearly 6-times that of 1P. Midday hours, when global irradiance is highest, demonstrate the most torque-tube-reflected light for both 1P and 2P systems. The frame sections perpendicular to the torque tube block torque-tube-reflected irradiance on the North and South edges of the module near the torque tube, and, in the 2P system, the frame adjacent and parallel to the torque tube shades the torque-tube-reflected irradiance. Frameless modules can therefore benefit more from torque tube reflection.

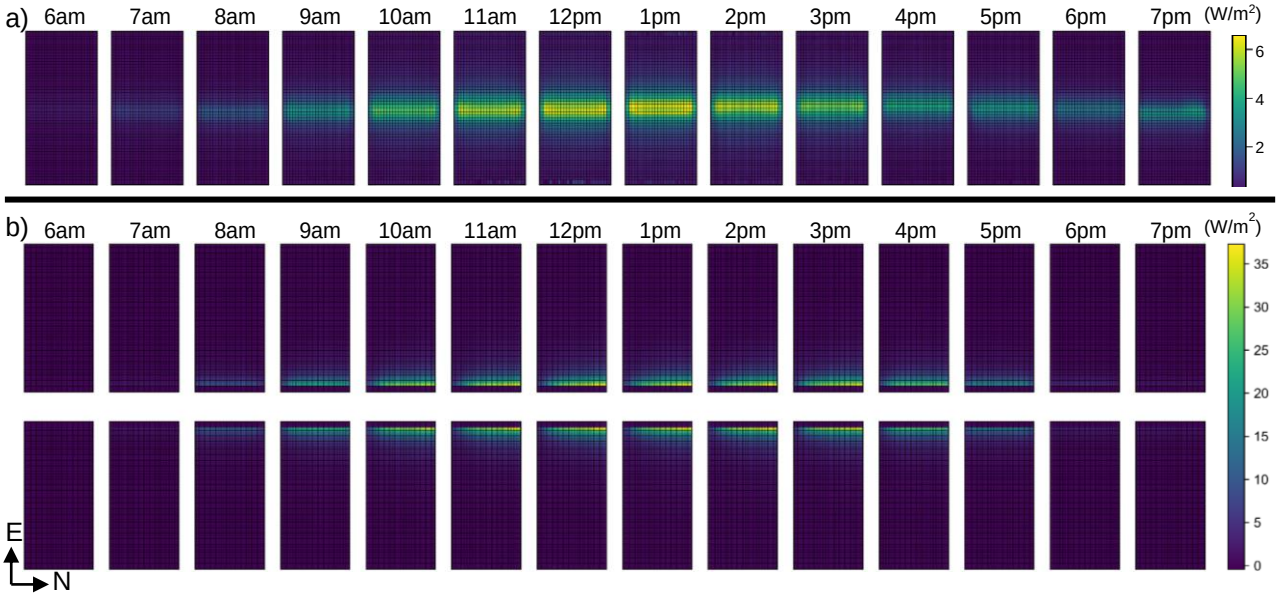

Figure 5. Average annual torque-tube-reflected irradiance maps for each non-zero irradiance hour in the day. (a) 1P and (b) 2P configurations. Note the difference in scales between (a) and (b).

3.3 Torque tube insolation fraction

The fraction of rear-side insolation contributed by torque tube reflection is given by

$$\text{Torque Tube Insolation Fraction [\%]} = \frac{\sum_{t=1}^{T} \bar{G}_{\text{TT}\,t}}{\sum_{t=1}^{T} \bar{G}_t} \quad (1)$$

where $\bar{G}_{\text{TT}_t}$ is the average module rear-side insolation due to torque tube reflection (Wh/m^2) and $\bar{G}_t$ is the average module rear-side insolation (Wh/m^2), for timestamp t out of T total timestamps. The average module rear side insolation is taken from the reflecting torque tube case, not the absorptive torque tube case.

For the 1P case, in Figure 6a, the proportion of rear-side irradiance contributed by torque tube reflection is flat at about 3% over the course of a day. Overall, despite minimal direct irradiance on the torque tube, the 1P module has a similar relative contribution of torque tube reflection to rear insolation as the 2P case at 0.6 albedo.

For the 2P case, in Figure 6b, the proportion of rear insolation from torque tube reflection is highest for the 0.2 albedo case due to reduced total rear-side irradiance. Direct light that passes through the torque tube gap onto the torque tube, and is reflected to the rear face remains constant with albedo. Thus, for smaller albedo, where there is less ground-reflected

irradiance and therefore less total rear irradiance, the torque tube reflection contributes a larger portion of the total rear irradiance.

Similarly, the fraction of rear-side irradiance contributed by the torque tube is highest in mid-morning and mid-afternoon for both albedos. In the first few hours of the day, the torque tube irradiance increases faster than the total rear-side irradiance. After mid-morning (around 9-10am), the torque-tube-reflected irradiance plateaus but the total rear-side irradiance continues to increase into midday. Therefore, despite the torque-tube-reflected irradiance being highest at solar noon, the fraction of rear irradiance contributed by the torque tube reflection exhibits a valley in the middle of the day and peaks in the late morning and evening hours; varying over this middle section of the day from 4.6%-7.2% and from 2.5%-4.4% for 0.2 albedo and 0.6 albedo, respectively, as shown in Figure 6b.

There is a higher fraction of total rear irradiance contributed by torque tube reflection on the eastern module in the morning, and on the western panel in the evening for both albedos (Figure 6b). This is due to reduced total rear irradiance on the eastern panel in the morning and on the western panel in the evening. As the module nearer to the ground, these modules receive less diffuse irradiance and therefore have smaller total rear irradiance. A smaller total rear irradiance results in a larger relative contribution from torque tube reflection.

Altogether, for an albedo of 0.6, torque tube reflection accounts for 2.9% and 3.1% of the annual rear insolation in 1P and 2P configurations, respectively. When the albedo is 0.2, torque tube reflection accounts for 3.0% and 5.5% of the annual rear insolation in 1P and 2P configurations, respectively. The relative contribution to 2P module rear insolation from torque tube reflection is higher for 0.2 albedo than for 0.6 albedo because there is a higher fraction of direct light in this case. A similar shift is not observed in the 1P case because no direct light hits the torque tube in the 1P configuration.

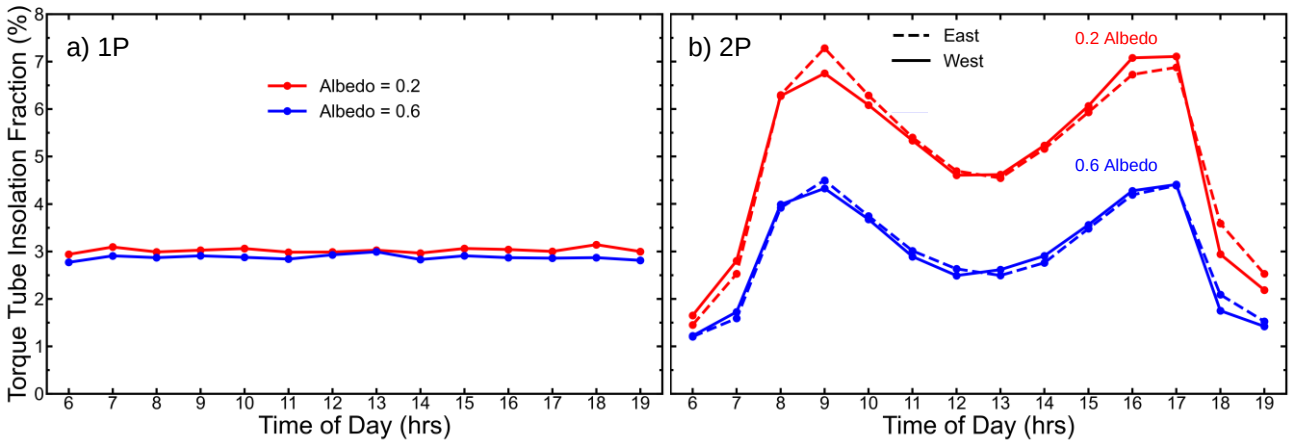

Figure 6. Average annual hourly fraction of total rear insolation due to torque tube reflection for (a) 1P and (b) 2P.

3.4 Hourly insolation mismatch

In addition to the total insolation added to the rear of the module by the torque tube reflection, the irradiance *distribution* across the module can also critically impact its performance. Irradiance mismatch is a measure of the spatial non-uniformity of the incident irradiance across a module at a given time. For a given timestamp *t*, the irradiance mismatch can be quantified by the mean absolute difference (MD) of irradiance across all irradiance calculation points.

$$MD_t\ [\mathrm{W/m^2}] = \frac{1}{n^2}\sum_{i=1}^{n}\sum_{j=1}^{n}\left|G_i - G_j\right| \tag{2}$$

where n is the number of total sample points on the modules, and G_i and G_j are the irradiance (W/m^2) at point i and point j, respectively [19]. We are investigating rear-side irradiance, but a similar approach can be taken for the front side. This instantaneous irradiance mismatch can vary widely over time, and translates to an instantaneous electrical loss in a non-linear relationship, as described in [20].

The relative mean absolute difference (RMD) in insolation provides a metric to compare irradiance mismatch between systems over T total timestamps and is given by:

$$RMD\ [\%] = \frac{\sum_{t=1}^{T} MD_t * \tau}{\sum_{t=1}^{T} \bar{G}_t} \tag{3}$$

where MD_t is the mean absolute difference between irradiance samples (W/m^2), τ is the timestamp duration (h), and, as above in Equation (1), $\bar{G}_t$ is the average module insolation (Wh/m^2), for timestamp t. This value is not directly equivalent to the total electrical mismatch loss over T total timestamps, and differs from the instantaneous irradiance of any one timestamp. Instead, it provides a measure of the irradiance spatial variation over one or multiple timestamps relative to the total insolation. RMD will be referred to as the rear insolation mismatch below.

Figure 7a shows the annual rear insolation mismatch of the 1P module under test with a reflective (triangles) and an absorptive (circles) torque tube, for 0.2 (red) and 0.6 (blue) albedo, by time of day. For both albedos, annual rear insolation mismatch is lower with the reflective torque tube than the absorptive torque tube, meaning that the torque tube reflection partially offsets the effect of torque tube shading in 1P modules. The difference in insolation mismatch (Figure 7b) is the impact of the torque tube reflection. Incorporating torque tube reflection decreases annual rear insolation mismatch by roughly 1% for both 0.2 and 0.6 albedo at every hour the day for the 1P case.

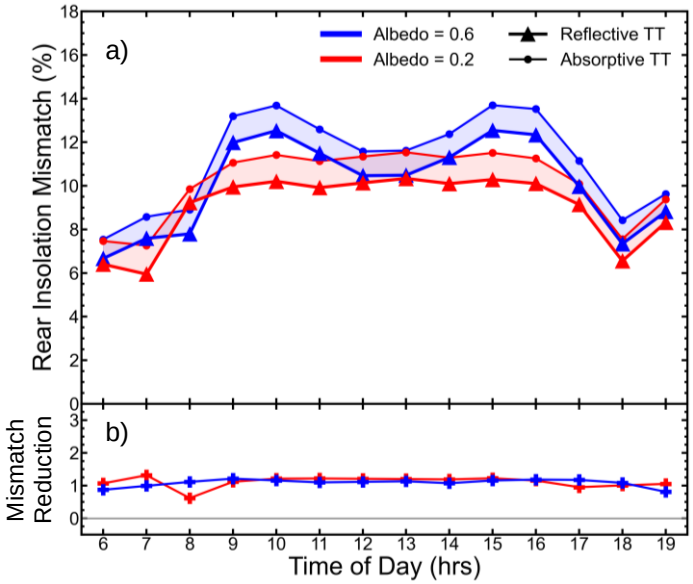

Figure 7. Rear insolation mismatch for the center module in a 1P array, as calculated in Equation (3), averaged over the year for each time of day. Both the reflective torque tube and absorptive torque tube cases are shown in (a); the difference (b) shows the effect of the torque tube reflection signal on rear insolation mismatch.

For the 0.2 albedo case, annual rear insolation mismatch is highest in the middle of the day. The mismatch does not dip down in the midday hours, as opposed to the 0.6 albedo case where the insolation mismatch peaks in the mid-morning and mid-afternoon (Figure 7a). The peaks in rear insolation mismatch for the 0.6 albedo case are due to one half of the module being tilted closer to the ground at these times, combined with the increased ground-reflected light at higher albedo, resulting in larger rear irradiance non-uniformities across the module length. Conversely, in the middle of the day when the module is near parallel to the ground, rear insolation mismatch is almost identical for 0.2 and 0.6 albedo.

Similar to the 1P module, torque tube reflection decreases annual rear insolation mismatch for 2P modules in both the 0.2 and 0.6 albedo cases (Figure 8a and Figure 8b, respectively). Insolation mismatch is higher for the eastern module (dashed lines) in the morning and the western module (solid lines) in the evening (i.e. the panel closer to the ground). As shown in Figure 8c and Figure 8d, the difference in total insolation mismatch on the 2P modules between the absorbing and reflecting torque tube cases varies throughout the day. This difference in insolation mismatch can even be negative for the 0.2 albedo case on the panel tilted higher in the sky, indicating torque tube reflection increases the rear insolation mismatch up to 0.6%. Although, at most times, the difference in insolation mismatch is positive and larger than in the 1P scenario; up to 2.9% and 2.0% for the 0.2 albedo and 0.6 albedo cases, respectively.

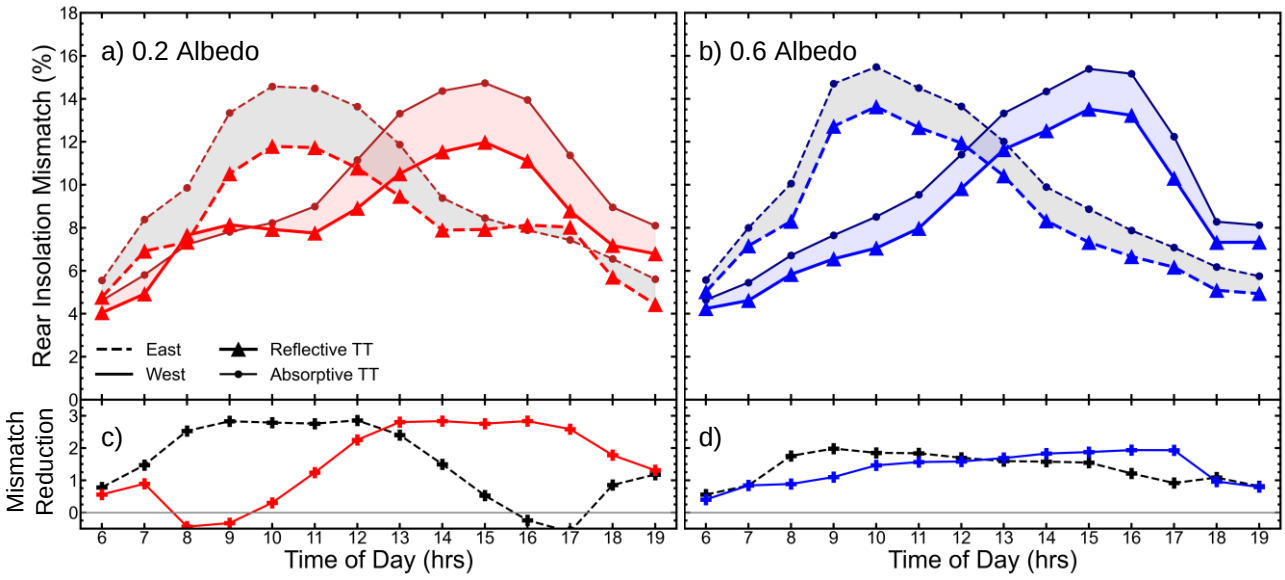

Figure 8. Rear insolation mismatch for the center module in a 2P array averaged over the year for each hour, for (a) 0.2 albedo, and (b) 0.6 albedo. Both the reflective torque tube and absorptive torque tube cases are shown; the difference is plotted in (c) and (d), demonstrating the impact of the torque tube reflection on rear insolation mismatch. Red: 0.2 albedo; blue: 0.6 albedo; dashed: eastern module; solid: western module.

3.5 Monthly fraction of rear insolation from torque tube reflection

Just as torque-tube-reflected insolation varies over the course of the day, it also varies over the course of the year. In Figure 9, the monthly torque tube insolation fraction is given for each month of the year for (a) the 1P system and (b) the 2P system, as calculated in Equation (1). For both the 1P and 2P systems, the 0.2 albedo case has a higher torque-tube-reflected insolation fraction than the 0.6 albedo case. This is due to lower total rear irradiance in the 0.2 albedo case, resulting in a larger torque-tube-reflected fraction of rear irradiance. In the 1P system, torque-tube-reflected light is primarily caused by diffuse and ground-reflected irradiance, and the fraction of rear insolation from torque tube reflection is relatively constant at around 3% for each month in the year. For the 2P system, where a large portion of torque-tube-reflected irradiance is caused by direct light, torque tube reflections contribute a higher fraction of total rear irradiance in the summer when direct irradiance is highest.

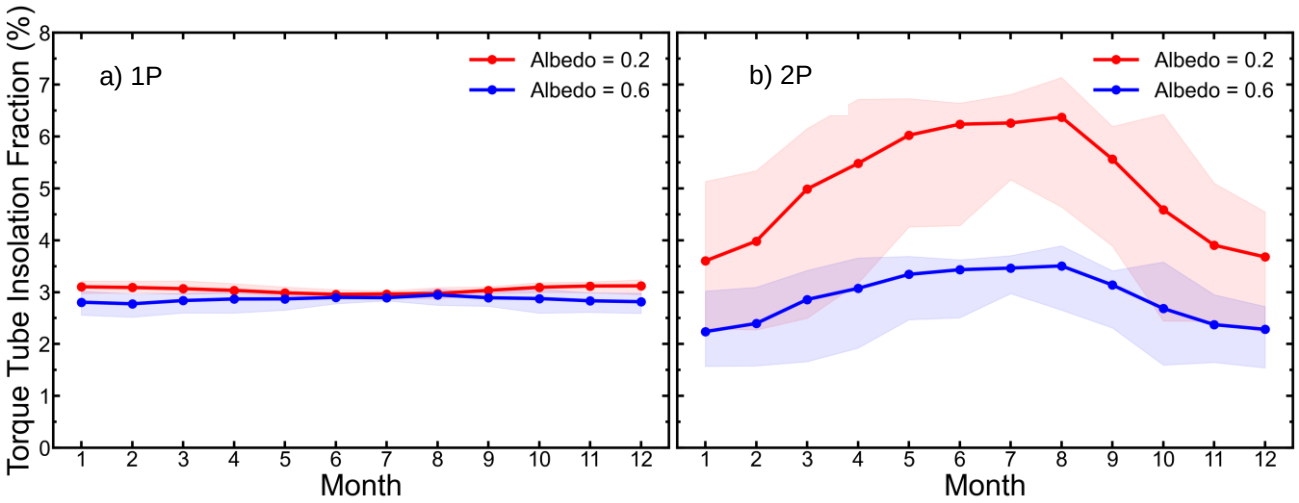

Figure 9. Monthly torque tube reflection insolation as a percentage of total rear insolation with a reflective torque tube for (a) 1P and (b) 2P modules. Curves indicate the average torque tube insolation fraction of all days for each month, and the colored bounds indicate the total range (minimum and maximum value) of daily torque-tube-reflected insolation fraction for each month.

Given the fraction of rear insolation from torque-tube-reflected light remains relatively constant in the 1P system for each month in the year (Figure 9a) and for each hour in the day (Figure 6a), bifacial energy yield models may be able to account for torque tube reflection in 1P systems as a constant factor. Conversely, the torque tube shadow affects 1P rear insolation mismatch on an hourly basis (Figure 7a), as shown by both the absorptive torque tube (circles) and the reflective torque tube (triangles). Thus, a detailed torque tube shading model must be considered to accurately predict rear-side insolation in 1P systems. However, the torque tube reflection reduces the rear insolation mismatch by an approximately constant value of 1% each hour of the day (Figure 7b), suggesting that a detailed shading model paired with a constant illumination factor may be sufficient to accurately calculate 1P bifacial yield. The same cannot be said for 2P systems because the fraction of rear insolation from torque-tube-reflected irradiance varies for each month in the year (Figure 9b) and for each hour in the day (Figure 6b).

4. CONCLUSIONS

In this work, we modelled the impact of incorporating a reflective torque tube on rear insolation and rear insolation mismatch for 1P and 2P SAT systems at the BiTEC site in Livermore, California. We demonstrated that torque-tube-reflected irradiance is focused near the torque tube, where torque tube shading is strongest. Torque tube reflection was shown to partially offset the effects of torque tube shading by increasing rear irradiance and decreasing rear-side irradiance mismatch in both 1P and 2P systems, and for both 0.2 and 0.6 albedos.

For the 1P system, torque tube reflection increased annual rear-side insolation by 3.0% and 2.9% for 0.2 albedo and 0.6 albedo, respectively, and reduced annual rear side insolation mismatch by 1.1% for both albedos. The torque-tube-reflected rear insolation fraction remained at 3% throughout the day, implying that the increase in rear irradiance due to torque tube reflection in 1P systems may be accounted for with a single correction factor. However, the hourly rear insolation mismatch varied hour by hour throughout the day from 5.9-10.3% and from 6.7-12.5% for 0.2 albedo and 0.6 albedo, respectively, due to torque tube shading. Therefore, for accurate 1P system bifacial energy yield prediction, torque tube shading should be accounted for on at least an hourly basis.

For a comparable 2P system, torque tube reflection increased annual rear insolation by 5.5% and 3.1% for 0.2 albedo and 0.6 albedo, respectively. In contrast to the 1P system, the 2P system's fraction of rear insolation from torque tube reflection rear insolation varied hour by hour throughout the day from 1.5-7.2% and from 1.2-4.5% for 0.2 albedo and 0.6 albedo, respectively, implying that torque tube reflection should be accounted for on at least an hourly basis instead of with a single correction factor. In addition, the 2P system's rear insolation mismatch varied hour by hour throughout the day from

4.1-12.0% for 0.2 albedo and from 4.2-13.6% for 0.6 albedo, indicating that torque tube shading should be accounted for on at least an hourly basis in the 2P system for accurate bifacial yield prediction, as in the 1P system. Incorporating torque tube reflection in the 2P system reduced the annual rear insolation mismatch by 1.5% and 1.7% for 0.2 albedo and 0.6 albedo, respectively, with some variation based on time of day, further suggesting 2P systems require torque tube reflection to be accounted for on at least an hourly basis.

We demonstrated that bifacial PV models that account for the effects of varying torque tube shading and reflections on an hourly basis can better represent real-world systems over the course of a day and year for both 1P and 2P systems. Unlike 2P systems, torque tube reflection in 1P systems may be simplified by applying a constant factor to the total rear irradiance.

REFERENCES

[1] "International Technology Roadmap for Photovoltaic (ITRPV) 2020 Results," in International Technology Roadmap for Photovoltaic" 12th edition, March 2021, <https://itrpv.vdma.org/documents/27094228/29066965/20210ITRPV/08ccda3a-585e-6a58-6afa-6c20e436cf41> (March 2021)

[2] M. Koussa, A. Cheknane, S. Hadji, M. Haddadi, and S. Noureddine, "Measured and modelled improvement in solar energy yield from flat plate photovoltaic systems utilizing different tracking systems and under a range of environmental conditions," Appl. Energy, 88(5), 1756–1771 (2011).

[3] C. D. Rodríguez-Gallegos et al., "Global Techno-Economic Performance of Bifacial and Tracking Photovoltaic Systems," Joule, 4(7), 1514–1541 (2020).

[4] R. Kopecek and J. Libal, "Towards large-scale deployment of bifacial photovoltaics," Nature Energy, 3, 443-446 (2018).

[5] J. Guerrero Pérez, I. Muñoz Benavente, and J. Navarro Berbel, "BiTEC Results 4 - Fall 2018 - Fall 2019: The Bifacial Year," Soltec, 2019, [Online]. Available: <https://lab.soltec.com/bifacial-trackers-ii/> (2019).

[6] J. S. Stein et al., "Bifacial Photovoltaic Modules and Systems: Experience and Results from International Research and Pilot Applications," Report IEA-PVPS T13-14 (2021).

[7] K. R. McIntosh, M. D. Abbott, B. A. Sudbury, and J. Meydbray, "Mismatch Loss in Bifacial Modules Due to Nonuniform Illumination in 1-D Tracking Systems," IEEE J. Photovoltaics, 9(6), 1504–1512, (2019).

[8] A. C. J. Russell, C. E. Valdivia, M. R. Lewis, J. E. Haysom, and K. Hinzer, "Modelling energy yield including rack shading for single-axis tracked bifacial solar panels," in 2019 Photonics North, 58891, (2019).

[9] S. A. Pelaez, C. Deline, J. S. Stein, B. Marion, K. Anderson, and M. Muller, "Effect of torque-tube parameters on rear-irradiance and rear-shading loss for bifacial PV performance on single-axis tracking systems," in 46th IEEE PVSC, vol. 2, pp. 3525–3530, (2019).

[10] S. Ayala Pelaez and C. Deline, "Bifacial_Radiance: a Python Package for Modeling Bifacial Solar Photovoltaic Systems," J. Open Source Softw., 5(50), 1865, (2020).

[11] S. A. Pelaez, C. Deline, S. M. Macalpine, B. Marion, J. S. Stein, and R. K. Kostuk, "Comparison of Bifacial Solar Irradiance Model Predictions with Field Validation," IEEE J. Photovoltaics, 9(1), 82–88, (2019).

[12] S. A. Pelaez, C. Deline, P. Greenberg, J. S. Stein, and R. K. Kostuk, "Model and Validation of Single-Axis Tracking with Bifacial PV," IEEE J. Photovoltaics, 9(3), 715–721, (2019).

[13] C. Deline, S. Macalpine, B. Marion, F. Toor, A. Asgharzadeh, and J. S. Stein, "Assessment of Bifacial Photovoltaic Module Power Rating Methodologies-Inside and Out," IEEE J. Photovoltaics, vol. 7, no. 2, pp. 575–580, (2017).

[14] G. W. Larson and R. A. Shakespeare, [Rendering with Radiance: The Art and Science of Lighting Visualization]. Morgan Kaufmann Publishers (1998).

[15] S. Crone, [Radiance Users Manual], vol. 2, (1992).

[16] J. Guerrero Pérez and J. Navarro Berbel, “BiTEC : How to simulate bifacial projects?,” Madrid, Spain, 2019, <https://lab.soltec.com/bifacial-trackers-ii/> (2019).

[17] T. Ribbon and T. R. Technology, “Tiger Bifacial DG Higher lifetime Power Yield,” 2015, <https://jinkosolar.eu/files/jinko/download/2020/datasheet/TR JKM445-465M-7RL3-BDVP-D4-EN.pdf> (2015).

[18] W. F. Holmgren, R. W. Andrews, A. T. Lorenzo, and J. S. Stein, “PVLIB Python 2015,” in 42nd IEEE PVSC, 1–5, (2015).

[19] C. Deline, S. Ayala Pelaez, S. MacAlpine, and C. Olalla, “Bifacial PV mismatch loss estimation and parameterization,” in 36th EU PVSEC, no. 1, 1–5, (2019).

[20] C. Deline, S. Ayala Pelaez, S. MacAlpine, and C. Olalla, “Estimating and parameterizing mismatch power loss in bifacial photovoltaic systems,” Prog. Photovoltaics Res. Appl., 28(7), 691–703, (2020).